Electronic Supporting Information

Regulation of Brønsted Acid Sites to Enhance the Decarburization of Hexoses to Furfural

Junbo Zhang,[a,b] Guoqiang Ding,[c] Yueqing Wang,[d] Fei Wang,[a] Hongxing Wang,[a,b] Yubo Liu,[a,b] Yulei Zhu,[a,c],* Yongwang Li[a,c]

[a] *State Key Laboratory of Coal Conversion, Institute of Coal Chemistry, Chinese Academy of Sciences, Taiyuan 030001, PR China*

[b] *University of Chinese Academy of Sciences, Beijing 100049, PR China*

[c] *Synfuels China Co. Ltd, Beijing 101407, PR China*

[d] *School of Energy and Power Engineering, North University of China, Taiyuan 030051, Shanxi, China*

* Corresponding authors. Tel: +86-010-6966 7798.

E-mail: zhuyulei@sxicc.ac.cn;

Experimental Methods

Sample Preparation

All the following organic and inorganic reagents were purchased from commercial suppliers and were used as received: $NaAlO_2$ (98%), NaOH (97%), HNO_3 (68 wt%) were all purchased from Beijing Chemical Co., Ltd. HF (40 wt%) were purchased from Sinopharm Chemical Reagent Co., Ltd. Silica sol (30 wt%) were purchased from Qingdao Haiyang Chemical Co., Ltd. Tetraethylorthosilicate (TEOS, 99%), tetraethylammonium hydroxide (TEAOH, 25 wt%), fructose (99%), glucose (99%) and soluble starch were all purchased from Aladdin. The commercial zeolite H-Beta-C (Si/Al = 12.5) was purchased from Nankai University Catalyst Co., Ltd.

Three methods were applied to prepare H-Beta zeolites with Si/Al ratio ranging from 5 to infinity, including seeding method, template method and template-seeding method. Seed-1 and Seed-2 were acquired from post-treatment of H-Beta-C, used for seeding method and template-seeding method, respectively. The former was given by calcination of H-Beta-C at 550 °C for 6 h while the later was given by complete dealumination of H-Beta-C based on the literature.[1]

Seeding method. Beta zeolite with Si/Al ratio of 5 was prepared by a template-free method with zeolite seed as a structure-directing agent. In a typical experiment, $NaAlO_2$ and NaOH were dissolved in H_2O to form a uniform aqueous solution. Then, silica sol was dropped into the above solution under stirring overnight. Afterwards, Seed-1 (seed/SiO_2 = 0.05) was added into the aluminosilicate gel with stirring vigorously for 5 min to give a final gel with composition of SiO_2:Al_2O_3:Na_2O:H_2O:Seed-1 = 1:0.059:0.269:11.34:0.05. The final gel was transferred to a Teflon lined stainless autoclave and was kept at 120 °C for 60 h under static conditions. The solid products were filtrated, washed and dried at 90 °C for 12 h to obtain parent Beta5.

Template method. Beta zeolite with Si/Al ratio of 10 and 15 were prepared by a conventional template method with TEAOH as structure-directing agent, following the previous literature.[2] The solid products acquired were filtrated, washed, dried and calcined at 550 °C for 8 h to give Beta10 and Beta15.

Template-seeding method. Beta zeolite with Si/Al ratio of 100, 200 and 400, as well as pure Si Beta zeolite (Si-Beta), were prepared by a combined template-seeding method, where both structure-directing agent and seed were used. Typically, a certain amount of $Al(OH)_3$ (or none) was added into TEAOH aqueous solution before TEOS was dropped, with stirring for 12 h. The above SiAl gel (or Si gel) was heated up to 60 °C and held for 3 h in order to evaporate ethanol. Next, Seed-2 (seed/SiO_2 = 0.04) was added into the gel with vigorous stirring for 5 min and HF aqueous solution was dropped to form a solid gel with a composition of

HF:(TEA)$_2$O:SiO$_2$:Al$_2$O$_3$:H$_2$O:Seed-2 = 0.53:0.27:1:x:13.36:0.04, where x was adjusted to the desired Si/Al ratio. The final gel was crystalized at 140 °C for 72 h and was then filtrated, washed and dried. Since no Na$^+$ or any other alkali metal ion was used in this synthetic system, H-type zeolites must be acquired by the simple calcination of the solid products. Therefore, H-Beta100, H-Beta200, H-Beta400 and Si-Beta must be acquired in this process.

Parent Beta5, Beta10 and Beta15 precursors were subject to ion exchange in NH$_4$Cl solution (1 mol/L) with a zeolite/solution ratio of 1/20 (g/mL) at 80 °C for 3 h. The operation was repeated twice to get NH$_4$-type samples. NH$_4$-type zeolites were then calcined at 550 °C for 6 h to give H-type zeolites.

Na-Beta15 samples were prepared through ion exchange of H-Beta5 following the literature.[3] Si-Beta@Al sample was prepared with impregnation of Al (NO$_3$)$_3$ solution on Si-Beta, followed by calcination at 550 °C for 4 h. DA-Si-Beta@Al was also prepared following the same method to Si-Beta@Al, with Seed-2 as precursor. The Al content in Si-Beta@Al or DA-Si-Beta@Al is same with H-Beta15.

Two control samples (H-Beta15-M and H-Beta-OH) were prepared by template-seeding method and dealumination, respectively. H-Beta15-M which has more intact morphology than H-Beta15 was prepared with H-Beta15 as seed. H-Beta15 was treated in nitric acid solution (2M) at 70 °C for 4 h to give H-Beta-OH that has the similar Si/Al ratio to H-Beta100 but has less hydrophobicity.

Catalytic evaluation

Fructose decarburization reaction was operated in an autoclave reactor. Because of the rapid consumption of carbohydrate at high temperature, the empty autoclave was pre-heated to the required temperature and then the substrate in a Teflon liner was quickly loaded to ensure the reaction run at the accurate temperature. Reaction conditions were as follows: 170 °C, 1.5 MPa (N$_2$), 1 g of fructose, 19 g of solvent (GBL/H$_2$O = 18/1) and 0.2 g of H-Beta zeolites. The concentrations of reactant and products were measured with an Agilent 1100 series high-performance liquid chromatograph (HPLC) equipped with a refractive index detector (RID), using a Shodex SH1821 column (8.0 mm × 300mm). 0.01 M of H$_2$SO$_4$ aqueous solution was used as mobile phase and the flow rate was 0.5 mL/min at a column temperature of 50 °C. The conversion and the selectivity were calculated as following:

$$\text{Conversion (mol\%)} = \frac{\text{mols of sugar}(inlet) - \text{mols of sugar}(outlet)}{\text{mol of sugar}(outlet)} \times 100\%$$

$$\text{Selectivity (mol\%)} = \frac{\text{moles of sugar converted to one product}}{\text{moles of sugar converted}} \times 100\%$$

Catalytic characterization

The X-ray powder diffraction (XRD) experiments were implemented on a Bruker D8 Advance diffractometer, using Cu Kα radiation (c = 1.5418 Å, 40 kV, 40 mA). The X-ray fluorescence spectroscopy (XRF) measurements were carried out on a Rigaku ZSX Primus II fluorescence spectrometer, to determine the Si/Al ratio.

The morphology of the samples was observed with a FEI QUANTA 400 field emission scanning electron microscope (SEM). Transmission electron microscopy (TEM) and high-resolution transmission electron microscopy (HRTEM) images were recorded using FEI (Talos^{TM} 200A) equipment with a voltage of 200 kV.

Brunauer–Emmett–Teller (BET) surface area was measured according to N_2 adsorption–desorption data acquired using a Micromeritics ASAP 2020 analyzer at −196 °C. Prior to the measurement, all samples were evacuated under vacuum at 350 °C for 8 h. The t-plot method was applied to obtain the micropore surface area and volume.

The acidity properties of the samples were investigated with *in situ* Fourier-transform infrared (FTIR) transmission spectrum of adsorbed pyridine and deuterated acetonitrile at 150 °C and 50 °C, respectively (Py-IR and CD_3CN-IR). It was performed on a Bruker TENSOR II spectrometer, ranging from 4000 to 850 cm^{-1} with a resolution of 4 cm^{-1}. Taking Py-IR for example, before measurement, about 25 mg of Beta zeolite was pretreated in vacuum at 500 °C for 1 h in the sample cell and then cooled to 150 °C to get a reference baseline signal. After that, Py-IR was introduced by the vacuum in sample cell and was kept for 30 min. Then the samples were heated up to 150 °C and was evacuated for another 30 min and infrared signal *vs.* the reference signal started to be recorded. CD_3CN-IR was conducted in the same way except for the operating temperature. To measure the IR spectra at hydroxyl region (OH-IR), 20 mg of zeolite powder was heated and degassed in a cell at 400 °C under vacuum for 2 h. The spectra were then collected at 150 °C.

The ^{27}Al and ^{29}Si magic angle spinning nuclear magnetic resonance spectra (MAS NMR) were obtained on Bruker Avance III HD spectrometer (600 MHz, B0 = 14.1 T) at a rotating frequency of 10 KHz at 25 °C. ^{27}Al MAS NMR spectra were recorded at a resonance frequency of 156.4 MHz with the excitation pulse length of 0.40 μs and the recycle time of 1 s. ^{29}Si MAS NMR spectra were recorded at a resonance frequency of 119.2 MHz with a pulse length of 2.0 μs and recycle time of 20 s.

Temperature programmed desorption of NH_3 (NH_3-TPD) was implemented on a Micromeritics Autochem II chemisorption analyzer to compare the total acid sites of the samples. The heating rate was 10 °C/min from

50 °C to 600 °C. The spent catalysts were carried out for Thermal analysis (TG/DTA) on a Shimadzu model DTG-60 instrument. For each run, 10 mg of sample was heated from 50 °C to 900 °C in an air flow at a heating rate of 10 °C/min.

In situ NMR analysis

In situ ^{13}C NMR of fructose conversion was recorded in NMR tube with adding D_2O in coaxial NMR tube as the lock signal. GBL/H_2O (H_2O = 5 wt%) mixture was employed as solvent and the concentration was lowered to 2 wt% to ensure complete dissolution of ([13]C-1)-D-fructose during the measurements of ^{13}C NMR. For quantitative analysis, the resonance peak at 69.4 ppm of γ-butyrolactone was employed as internal standard.
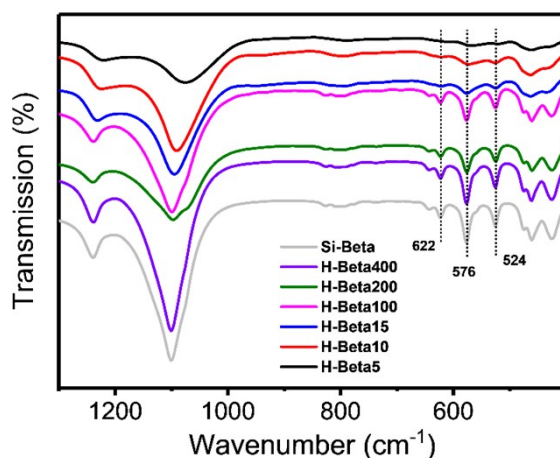
Fig. S1 FT-IR spectra of skeletal vibration of H-Beta zeolites with different Si/Al ratios.

Three characteristic peaks of Beta zeolite centered at 524 cm^{-1}, 576 cm^{-1} and 622 cm^{-1} were observed for all the samples. Therein, the band at 576 cm^{-1} refers to IR vibration of the double five-membered ring and was usually taken as the indicator of crystallinity. From H-Beta5 to Si-Beta, the intensity of this band holds a huge enhancement which is in accordance with XRD patterns. The IR peak at around 950 cm^{-1} belonging generally to internal defect sites is absent for high-Si zeolites. The band at 1000–1200 cm^{-1} represents the T-O-T asymmetrical stretching vibration of zeolites, which shifts from 1074 cm^{-1} to 1101 cm^{-1} as the Si/Al ratio increases from 5 to infinity, according with previous researches.[4, 5]
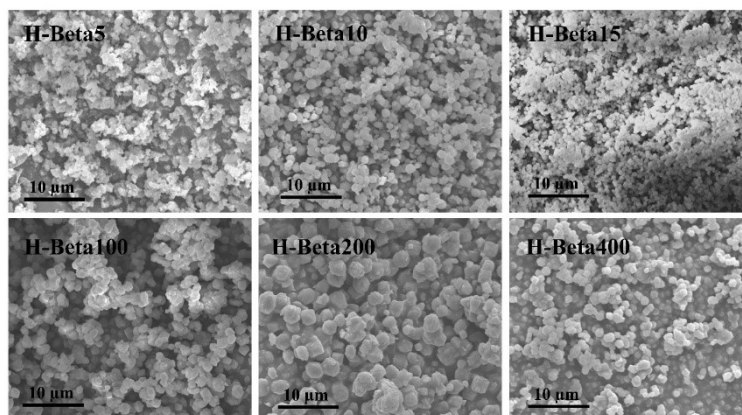
Fig. S2 SEM images of zeolite Beta with different Si/Al ratio.
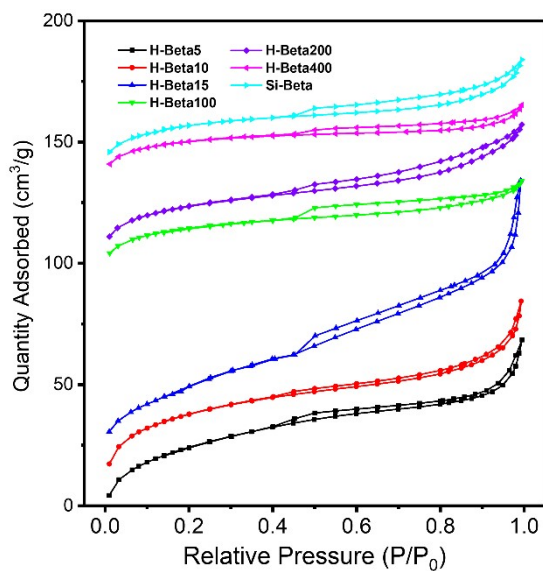
Fig. S3 Adsorption–desorption isotherms of N_2 at low temperature for H-Beta zeolites.
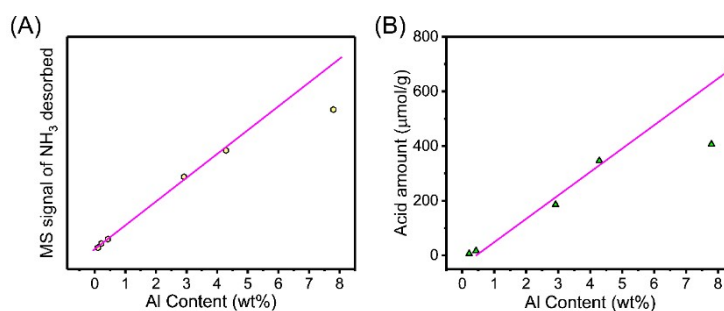
Fig. S4 Correlations of acid amount with Al content for H-Beta zeolites obtained from (A) NH_3-TPD and (B) Py-FTIR.
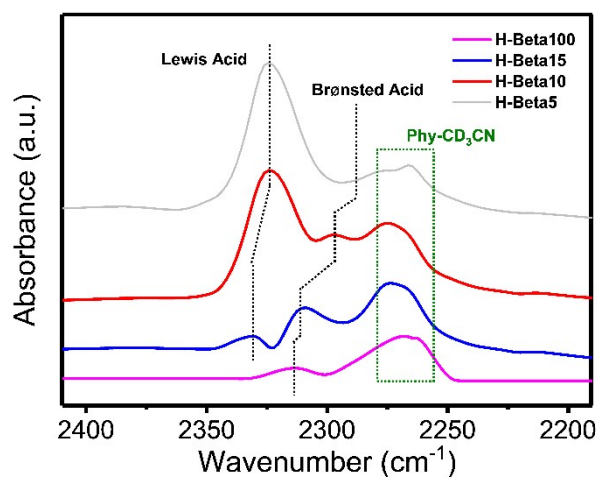
Fig. S5 FT-IR spectra of d3-acetonitrile adsorbed on H-Beta zeolites after saturation followed by evacuation for 1 min.
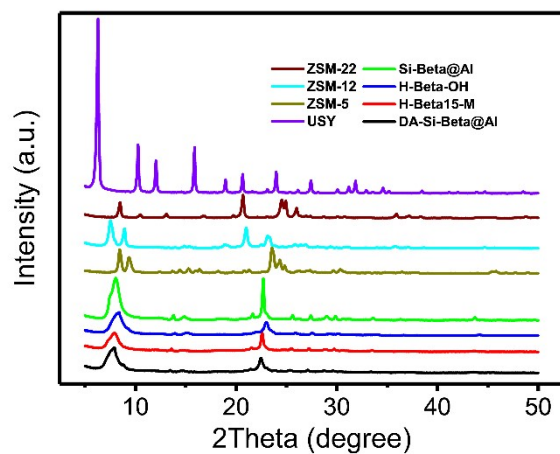
Fig. S6 XRD patterns of various samples.
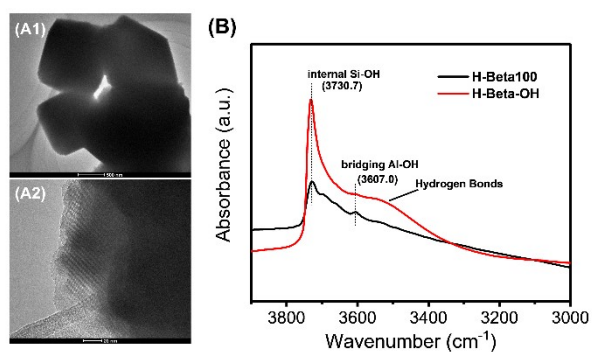
Fig. S7 (A) TEM and HRTEM images of H-Beta15-M and (B) FT-IR spectra in hydroxyl-stretching region of H-Beta100 and H-Beta-OH.
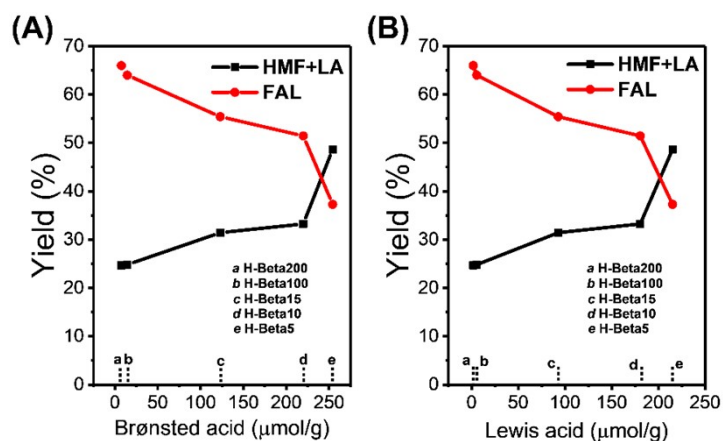
Fig. S8 Correlations between product yield and (A) Brønsted acid and (B) Lewis acid.
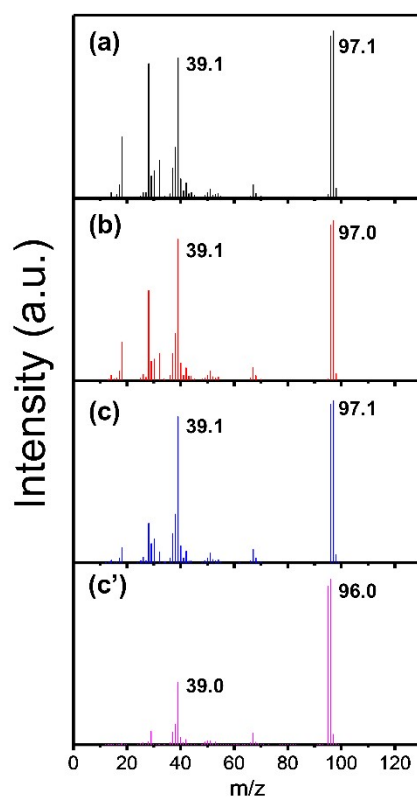
Fig. S9 The mass spectra of furfural in substrate when using [^{13}C-1]-fructose as reactant: (a) H-Beta5, (b) H-Beta15 and (c) H-Beta200. (c') unlabeled fructose as reactant on H-Beta200.
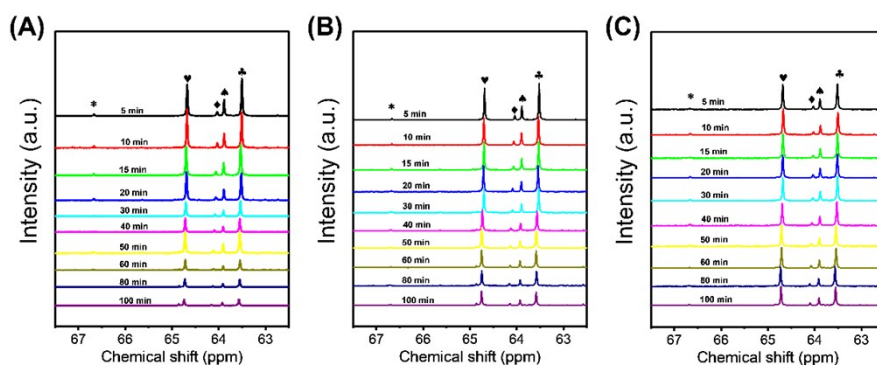
Fig. S10 *In situ* ^{13}C NMR spectra as a function of time for the conversion of [[13]C-1]-fructose over H-Beta zeolites at 170 °C. (A) H-Beta5, (B) H-Beta15 and (C) H-Beta200. Fructose isomers: (*) keto, (♥) β-pyranose, (♦) α-pyranose, (♠) α-furanose and (♣) β-furanose.
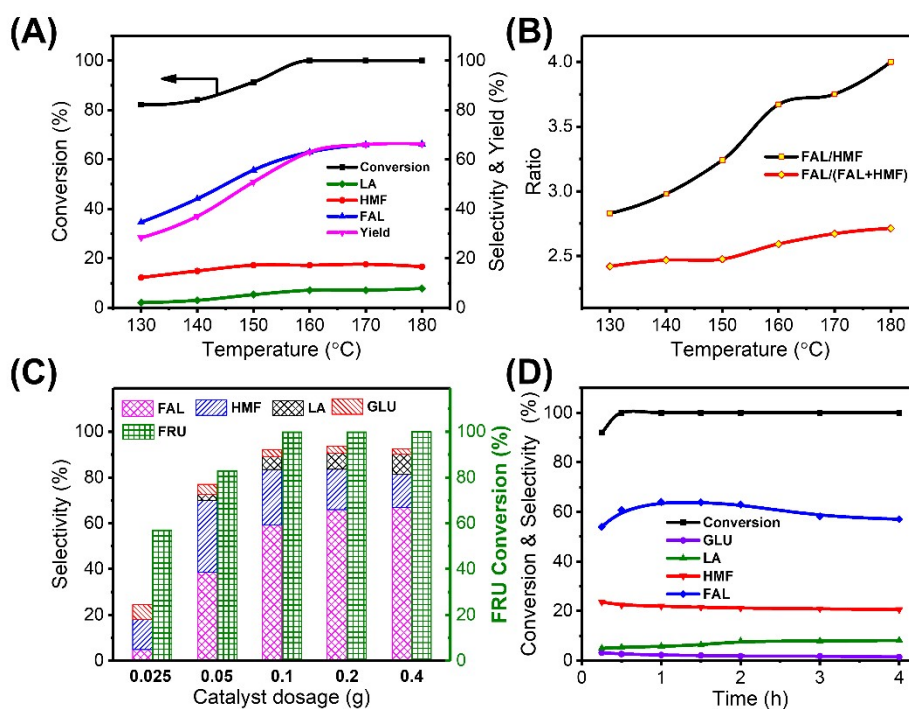
Fig. S11 The effect of reaction temperature (A) and (B) on FRU decarburization over H-Beta200. The effect of catalyst dosage (C) on FRU decarburization over H-Beta200. (D) The evolution curves of FRU decarburization with time. Reaction conditions: 18 g GBL, 1g H_2O, 1 g fructose, 0.2 g catalyst; 170 °C; 1 MPa N_2. (FRU=fructose, GLU=glucose).

FAL and HMF are the two main products obtained in this reaction, where the former is generated from C–C bond fracture and the latter stems from direct dehydration. HMF may undergo further hydration, giving levulinic acid accompanied by one molecule of formic acid. To optimize the reaction conditions, we systematically investigate the influence of reaction temperature and catalyst dosage on fructose decarburization. As depicted in Fig. S11, fructose conversion increases progressively with increasing

temperature and full consumption was achieved at 160 °C. In particular, temperature presents an obvious promoting effect on furfural generation. One explanation may lie in the fact that high temperature is more beneficial to the thermal diffusion of fructose from external into the internal pores of zeolites, which improves the odds of C–C bond fracture and hence favors the production of fructose. In comparison, parallel product of HMF hasn't changed obviously (Fig. S11A). To ascertain the promotion degree of temperature effect on different products, the correlation of FAL/HMF ratio *vs.* temperature was established (Fig. S11B). Significantly, the ratio of FAL/HMF increases with temperature although both FAL and HMF benefit from temperature effect. This suggests that the increase of temperature is more profitable to FAL than HMF. Even though LA was involved, the ratio of FAL/(HMF+LA) still presents positive correlation. The above results clarified that ΔE_{FAL} (activation energy) is larger than ΔE_{HMF} in terms of dynamics.

Fig. S11C shows the effect of catalyst dosage on the performance of fructose conversion over H-Beta200 at 170 °C. As well-known, it would be more prospective if a batch reaction could be achieved at a low catalyst concentration. However, reducing cost in the expense of product selectivity is undesirable. As can been seen, a low FAL yield of 2.81% was obtained with a catalyst dosage of 0.025g and fructose conversion is only 57.2%. With the increase of catalyst amount, a simultaneous improvement was found for conversion and FAL selectivity. At the catalyst dosage of 0.2g, full conversion was accomplished with a FAL yield of 66.0%. When the amount of the catalyst further increased, FAL yield remained almost unchanged while HMF yield significantly dropped from 17.6% to 14.3%. This suggests the better stability of FAL against degradation than HMF.
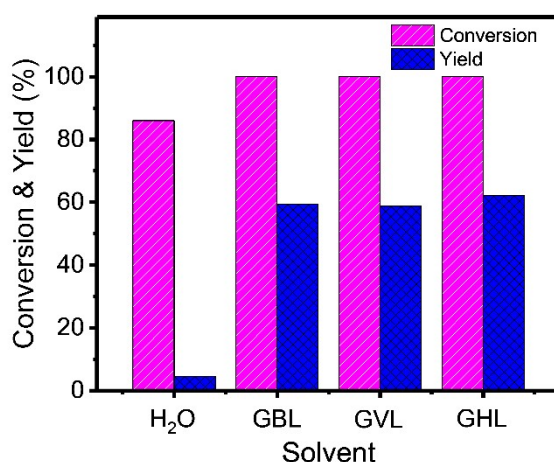
Fig. S12 Comparison of fructose conversion in various solvents. Reaction conditions: 18 g solvent, 1g H_2O, 1 g fructose, 0.2 g catalyst; 170 °C; 1 MPa N_2; 1 h. (GVL: γ-valerolactone; GHL: γ-hexalactone).

For carbohydrate transformation catalyzed by solid acid, solvent effect is extremely obvious in many ways including enhancing solubility of reactants, inhibiting degradation of products and promoting interaction of solvent and active center. Using GBL as the solvent in the decarbonization of fructose to FAL, it was reported that cooperative effect between acid center of Beta zeolite and GBL accelerates the selective fracture of C-C bond in fructose, which greatly improves the furfural yield.[6] To further study the unique role of lactones, GBL, GVL and GHL were employed as displayed in Fig. S12. All the three lactones achieved total conversion in 1 hour of reaction but solvent water gave an incomplete conversion and an extremely low FAL yield. This is attributed to the severe side reactions initiated by water, in which carbohydrates and furfural derivatives could not stabilize generally. Compared to GBL and GVL, GHL exhibited a little more FAL yield although there is no too much difference in the structures of the three molecules. In terms of molecule properties, both GBL and GVL are water-soluble while GHL is water-insoluble. This inspires up to extrapolate that the higher FAL yield for GHL may be ascribed to poor water-solubility, which drives furfural from aqueous phase into organic phase and therefore suppresses FAL degradation.[7] Even so, the high price makes GHL difficult for now to apply at a large scale.
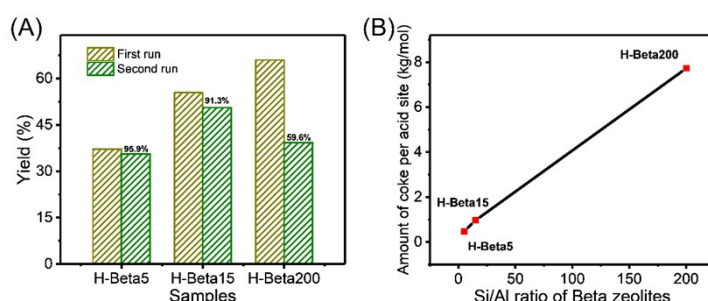
Fig. S13. (A) Catalytic performances over H-Beta zeolites for the first and the second run. Reaction conditions: 18 g GBL, 1g H_2O, 1 g fructose, 0.2 g catalyst; 170 °C; 1 MPa N_2; 1 h. (B) Correlation between the amount of coke per unite of acid site and the Si/Al ratio of H-Beta zeolites.

Table S1. The proportions of each type of Al species for H-Beta zeolites.

Samples	Proportion (%)[a]				Al_F/Al_{NF}
	$^{IV}Al_F$	$^{V}Al_{NF}$	$^{VI}Al_{NF}$	D-$^{VI}Al_{NF}$	
H-Beta5	62.0	9.6	28.4	0	1.63
H-Beta15	76.5	0	12.8	10.7	3.26
H-Beta200	100	0	0	0	+∞

[a] The results were calculated from deconvolution of ^{27}Al MAS NMR spectra.

Table S2. The main characterizations of various samples.

Samples	Si/Al ratio[a]	Specific surface area (m$^2 \cdot$g^{-1})[b]		Pore volume (cm$^3 \cdot$g^{-1})[b]	
		Total	Micropore	Total	Micropore
USY	20.6	674.5	588.2	0.48	0.29
ZSM-12	39.3	301.2	208.1	0.21	0.10
ZSM-5	13.2	337.6	250.0	0.19	0.12
ZSM-22	37.5	255.6	180.3	0.15	0.07
Si-Beta@Al	16.6	427.7	378.3	0.23	0.19
DA-Si-Beta@ Al	14.7	446.2	322.1	0.45	0.16
H-Beta15-M	15.4	482.5	365.8	0.38	0.23
H-Beta-OH	137.3	540.7	358.3	0.57	0.17

[a] Determined from XRF. [b] Determined from low-temperature N$_2$ adsorption–desorption.

Table S3. Catalytic performance of the other samples at 170 °C.[a]

Catalyst	Sugar	Conversion (%)	Selectivity (%)		FAL/HMF
			HMF	FAL	
H-Beta-C	fructose	100	22.5	52.0	2.31
H-Beta200	arabinose	55.3	–	86.4	–

[a] Reaction conditions: 18 g GBL, 1g H$_2$O, 1 g fructose or 0.83 g arabinose, 0.2 g catalyst; 170 °C; 1 MPa N$_2$; 1 h.

Table S4. Comparison of catalytic performances of fructose decarburization over various catalysts.

Catalyst	Temp. (°C)	FAL yield (%)	Ref.
H-Beta200 zeolite	170	66.0	This work
mordenite zeolite	175	36.0	8
Beta zeolite	150	63.5	6
ZSM-5 zeolite	150	63.0	9
Y zeolite	150	37.8	10
Beta zeolite	150	50.3	11
Beta zeolite	170	51.8	12

References

1. X. Yang, Y. Liu, X. Li, J. Ren, L. Zhou, T. Lu and Y. Su, *ACS Sustainable Chemistry & Engineering*, 2018, **6**, 8256-8265.
2. X. Zeng, Z. Wang, J. Ding, L. Wang, Y. Jiang, C. Stampfl, M. Hunger and J. Huang, *J. Catal.*, 2019, **380**, 9-20.
3. H. Xia, H. Hu, S. Xu, K. Xiao and S. Zuo, *Biomass and Bioenergy*, 2018, **108**, 426-432.
4. S. Chu, L. n. Yang, X. Guo, L. Dong, X. Chen, Y. Li and X. Mu, *Molecular Catalysis*, 2018, **445**, 240-247.
5. W. Wang, W. Zhang, Y. Chen, X. Wen, H. Li, D. Yuan, Q. Guo, S. Ren, X. Pang and B. Shen, *Journal of Catalysis*, 2018, **362**, 94-105.
6. J. Cui, J. Tan, T. Deng, X. Cui, Y. Zhu and Y. Li, *Green Chemistry*, 2016, **18**, 1619-1624.
7. P. Bhaumik and P. L. Dhepe, *ACS Catalysis*, 2013, **3**, 2299-2303.

8. E. I. Gurbuz, J. M. Gallo, D. M. Alonso, S. G. Wettstein, W. Y. Lim and J. A. Dumesic, *Angew Chem Int Ed Engl*, 2013, **52**, 1270-1274.

9. L. Wang, H. Guo, Q. Wang, B. Hou, L. Jia, J. Cui and D. Li, *Molecular Catalysis*, 2019, **474**.

10. L. Wang, H. Guo, Q. Xie, J. Wang, B. Hou, L. Jia, J. Cui and D. Li, *Applied Catalysis A: General*, 2019, **572**, 51-60.

11. Y. Wang, G. Ding, X. Yang, H. Zheng, Y. Zhu and Y. Li, *Applied Catalysis B: Environmental*, 2018, **235**, 150-157.

12. Y. Wang, X. Yang, H. Zheng, X. Li, Y. Zhu and Y. Li, *Molecular Catalysis*, 2019, **463**, 130-139.